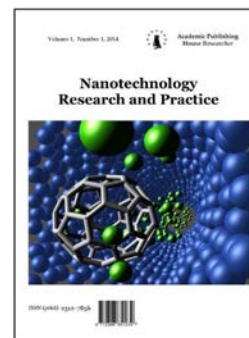


Copyright © 2015 by Academic Publishing House *Researcher*

Published in the Russian Federation  
Nanotechnology Research and Practice  
Has been issued since 2014.  
ISSN: 2312-7856  
Vol. 6, Is. 2, pp. 60-67, 2015

DOI: 10.13187/ejnr.2015.6.60

[www.ejournal13.com](http://www.ejournal13.com)

UDC 537.311.33

## Effects of the Magnetic Flux and the Rashba and the Dresselhaus Interactions on the Tunneling Nanoscale Magnetoresistance of a Three-Terminal Quantum Ring

<sup>1</sup>Mostafa Behtouei<sup>2</sup>Amin Maleki Sheikh Abadi

<sup>1</sup>University of Rome "ROMA TRE", Italy  
Faculty of Engineering

<sup>2</sup>University of Rome "ROMA TRE", Italy  
Faculty of Physics

### Abstract

In this paper we investigated the effect of tunneling magnetoresistance in one-dimensional three-terminal mesoscopic ring in the presence of the magnetic flux and the Rashba spin-orbit interaction (RSOI) and the Dresselhaus spin-orbit interaction (DSOI). We calculated the current flow in this structure based on the Landauer-Buttiker formalism and a generalized Green's function technique for parallel and antiparallel spin orientations in ferromagnetic electrodes. Calculations show that the tunneling magnetoresistance increases with the strength of the magnetization. The required conditions for reach the maximum values of the tunneling magnetoresistance are also calculated.

**Keywords:** tunneling magnetoresistance, three-terminal mesoscopic ring, magnetoresistance, Rashba, Dresselhaus.

### Introduction

The magnetic properties of nanoscale magnets and manipulation of electron spin degree of freedom have been the focus of intensive research in the past few decades for both fundamental physics and attractive potential applications [1, 2]. During the rapid development of nanotechnology, much attention has been paid on the spin injection and the tunneling magnetoresistance (TMR) effect in tunnel junctions made of semiconductor spacers, sandwiched between ferromagnetic leads [3]. The magnetoresistance exhibits a strong dependence on the relative magnetization directions in these layers and on their spin polarizations [4–8]. Its new characteristics, for example, anomalies of the TMR caused by the intra-dot Coulomb repulsion energy, were analyzed in the subsequent theoretical work based on the non-equilibrium Green's function method [9]. Also, numerous investigations relate to the transmissions, conductances, and traversal times [10–12]. Spintronics devices based on the TMR effect in magnetic multi-layers, such as magnetic field sensor and magnetic hard disk read heads have been used as commercial products, and have greatly influenced the current electronic industry. Some successful attempts have been already made in this direction, based on the use of ferromagnetic metal or combined magnetic and non-magnetic semiconductor contacts [13]. In such devices based on the spin polarization of the current inject from the ferromagnetic leads which can be effectively tuned by the magnetic flux and the Rashba spin-orbit interaction (RSOI) and the Dresselhaus spin-orbit

interaction (DSOI). The component of two types of SOIs, the Rashba [14] and the Dresselhaus [15], is a novel and crucial tool in modulating the electron transports and spin precessions in some typical materials [16–20]. Therefore, the SOIs play a very important role in the electron transport of Spintronic devices, such as spin field effect transistor (SFET). Meanwhile, the constitution of the magnetic tunnel junction (MTJ) also has significant effects in controlling the spin electron transport [21]. The TMR has the expectation of realizing the applications of novel tunneling-based Spintronic devices, such as hard disk drives, magnetic field sensors, and magneto-resistive random access memory, the magnetic properties of nanoscale magnets have been the focus of intensive research in the past few decades both experimentally and theoretically [22–25]. The TMR effect was first observed by M. Julliere [26] in 1975, where was measured the change in electrical resistance on switching the relative alignment of the Fe and Co magnetic moments from parallel to antiparallel in Fe/Ge–O/Co MTJ structure. In such a system, both of the RSOI and DSOI exist simultaneously and behave like in-plane momentum-dependent effective magnetic fields. In fact, these fields add spin-dependent geometric phases to the electron wave function in semiconductor quantum rings. The Aharonov-Bohm [27] (AB) effect and its relativistic counterpart, the Aharonov-Casher (AC) [28] effect, are just two of these quantum interference phenomena that may appear simultaneously. The Aharonov-Bohm (AB) phase represents the geometric phase acquired by the orbital wave function of the charged particle encircling a magnetic flux line. This phase is experimentally well established and manifests itself through oscillations in the resistance of mesoscopic rings as a function of an external magnetic field. The spin part of the particle's wave-function can acquire an additional geometric phase in the systems with strong spin-orbit interactions [29, 30]. Spin sensitive quantum interferences under the influence of the AB and AC effects make the quantum rings to have a practical significance for designing nano-electromagnetic spin devices, such as spin switches [31, 32], detectors [33], spin transistors [34], filters [35], and scalable devices for quantum information processing. Generally, the tunneling probability of the electron flowing through the mesoscopic rings depends on few factors: (i) the relative orientations of the electrode magnetizations, which can be changed from the parallel (P) to anti-parallel (AP) by applying an external magnetic field; (ii) the RSOI and DSOI strength; (iii) the effects of relative positions of the drain electrodes in quantum ring; (iv) the coupling strength between the leads to the ring; (v) Fermi energy of transmission electrons; (vi) the semiconductor size (number of sites in the ring) [36–39]. In this paper, by solving the related equations, we aim to show the effects, such as SOIs combination, magnetic flux, and the required conditions for reach the maximum values of the tunneling magnetoresistance. In our opinion, the current flow in a quantum ring exists a possibility of making real progress in using the parallel and antiparallel spin orientations in ferromagnetic electrodes in special value of the magnetic flux and the Rashba spin-orbit interaction (RSOI) and the Dresselhaus spin-orbit interaction (DSOI). The relative orientation of the magnetization of ferromagnetic electrodes and SOIs can affect dramatically electron transport across a tunneling barrier connecting them. Therefore, this makes the TMR properties to be strongly affected by the spin accumulation and magnetoresistance. The paper is organized as follows. The model systems are introduced and related basic formulations are shown in Section II. Details of the calculation procedure affected by the magnetization, the SOIs combination, and strength of both RSOI and DSOI are described and analyzed thoroughly in Section III. In Section IV the corresponding conclusions are presented.

### Model and formulations

We considered a mesoscopic ring with three leads and mapped onto a one-dimensional virtual lattice with a symmetric geometry of leads, i.e.  $\varphi_1 = \varphi_2 = \varphi_3 = 120$  ( $\varphi$  is an angle between leads). The right leads act as a source ( $s$ ) that is ferromagnetic materials in all stages of the calculation and the two left leads act as drains ( $d_1$  and  $d_2$ ), which we consider them being in two states of ferromagnetism material and antiferromagnetism material. In the tight-binding model, an electron can jump from one site to the nearest neighbor sites with a hopping energy matrix  $[t]$ . The total Hamilton,  $\bar{H}$ , with regard to the transport of coherent electron jumps between the nearest neighbor sites can be written as:

$$\bar{H} = H + H_q \quad (1)$$

where,  $H$  – is the Hamiltonian of isolated ring and  $H_p$ , with  $P = s, d_1, d_2$  – is the Hamiltonian due to the coupling between the ring and the source lead, up drain lead, and down drain lead, respectively. Therefore, the total Hamiltonian is the sum of the contribution of the ring,  $H$ , and  $H_p$  with  $P = s, d_1, d_2$ . In this paper, we consider a source consists of the ferromagnetism materials and two drains electrodes are in two state ferromagnetism and antiferromagnetism. In the absence of the electron-electron and electron-phonon interaction,  $H$ , can be written as follows:

$$H = \sum_{i=1}^N (\epsilon_i c_i^\dagger \sigma_0 c_i - c_i^\dagger [t] e^{i\alpha} c_{i+1} - c_{i+1}^\dagger [t]^\dagger e^{-i\alpha} c_i) \quad (2)$$

here,  $[t]$  – is a matrix  $2 \times 2$  which is given by [40–41]

$$[t] = t\sigma_0 + i[t^R \cos \beta_i - t^D \sin \beta_i] \sigma_x + i[t^R \sin \beta_i - t^D \cos \beta_i] \sigma_y \quad (3)$$

In,  $\beta_i = \frac{\pi}{N}(i - 1/2)$ ,  $\beta_i$  – periodic boundary condition is imposed by  $3N + 1 = 1$  and values of atomic sites ( $3N$ ) on the ring are equal to 100. The Peierls phase factor  $e^{i\alpha}$  with  $(2\pi/3N)\varphi/\varphi_0$  describes the influence of the magnetic field in terms of the magnetic flux,  $\varphi$ , threaded by the ring, and  $\varphi_0 = hc/e$  is the flux quantum and  $\epsilon_i$  is Anderson-like on site disorder energy strength. The  $t^R$  and  $t^D$  are RSOI and DSOI strength, respectively, and  $\sigma_0$  is the  $2 \times 2$  identity matrix in the spin space. Here,  $t$  – is intensity jumps between nearest neighbor sites that in this paper, we put it equal to one. The Hamiltonian due to the coupling between the ring and the source lead and output leads can be written as:

$$H_p = \sum_{p=s,d_1,d_2} t_p \sum_{i=1}^{\infty} (\epsilon_i^\dagger b_i^\dagger \sigma_0 b_i - \delta_{i,1} b_i^\dagger \sigma_0 c_{ip}) \quad (4)$$

In the two component operator,  $c_i^\dagger = (c_{i\uparrow}^\dagger, c_{i\downarrow}^\dagger)$ ,  $c_{i\sigma}^\dagger (c_{i\sigma})$  – is the creation operator (annihilates) of an electron on the site  $i$  with spin-state. We consider that the linear transport regime conductance  $G$  of the interferometer can be obtained using the Landauer conductance formula [42]:

$$G_\sigma = \frac{2e^2}{h} T_{pq}^{\sigma\sigma} \quad (5)$$

where,  $T_{pq}^{\sigma\sigma}$  – is the transmission probability of an electron across, it can be expressed in terms of Green's function and its coupling to the side-attached electrons by [43]:

$$T_{pq}^{\sigma\sigma'} = \text{Tr}[\Gamma_p^\sigma G \Gamma_q^{\sigma'} G^\dagger] \quad (6)$$

Here,  $G$  – is Green's function and the coupling of the source and drains described by  $\Gamma_p^\sigma$  and  $\Gamma_q^{\sigma'}$ :

$$\Gamma_p = i(\Sigma_p - \Sigma_p^\dagger); \quad \Sigma_p = -t_p e^{ik_0 a} \sigma_0 \quad (7)$$

The coherent transport is then calculated using the Landauer's formula and the retarded Green's function of the ring is computed as:

$$G_c = (E^+ - H_c - \Sigma_p \Sigma_p)^{-1} \quad (8)$$

where  $E^+$  – is complex energy for one way to incorporate the boundary into the equation and self-energy  $\Sigma_p$  describes the effect of the leads on the conductor of  $\Sigma_p$  with  $p=s, d_1, d_2$  and it calculated by  $\Sigma_p t_p^\dagger g_p t_p$ , where  $t_p = -t_0 \sigma_0$  and  $k_0$  satisfies the relation  $E = M - 2t_p \cos k_0 a$ , hence the conductance of the ring finally obtains as the Landauer equation ( $M$  is the intensity of magnetization). Therefore, the tunneling magnetic resistance (TMR) is calculated as follows:

$$TMR = \frac{(G_\sigma^F + G_\sigma^P) - (G_\sigma^{AF} + G_\sigma^A)}{(G_\sigma^F + G_\sigma^P)} \quad (9)$$

where  $G_\sigma^{AP}$  and  $G_\sigma^P$  – are the conductivity in the ferromagnetic state (P) and in the antiferromagnetic state (AP), respectively.

### Results and discussion

In linear response, the tunnel magnetoresistance is defined as a relative change in the conductance of the system when the magnetizations of the two ferromagnetic layers switch between parallel (P) and antiparallel (AP) configurations, hence:  $TMR = \frac{(G_\sigma^P - G_\sigma^{AP})}{G_\sigma^P}$ . Conductance itself is simply calculated as a derivative of the current with respect to magnetization intensity ( $M$ ) where,  $G_\sigma^{AP}$  and  $G_\sigma^P$ , respectively, the conductivity in the ferromagnetic state (P) and antiferromagnetic state (AP), where:  $G_\sigma^P = G_{\uparrow\uparrow} + G_{\downarrow\downarrow}$  and  $G_\sigma^{AP} = G_{\uparrow\downarrow} + G_{\downarrow\uparrow}$  (the arrows denote the

orientations of magnetization of the electrodes). It should be also mentioned that our calculations are based on the assumptions of coherent and elastic transport, for which the current conservation rule is fulfilled at each sites of rings. In all figures in this paper, we compare to the effect SOIs and magnetization intensity with values of TMR. Here, Spin-orbit coupling strengths can be written [44] as  $t^R = \alpha/2a$  and  $t^D = \beta/2a$ , where  $\alpha$  is the strength of the RSOI,  $\beta$  is the strength of the DSOI, and  $a$  is the lattice spacing constant. The Dresselhaus spin-orbit interaction (DSOI) induced by bulk inversion asymmetry (like zinc-blend structure) and usually is fixed for a given material. However, the Rashba spin-orbit interaction (RSOI) is induced by the structure inversion asymmetry. The strength of the RSOI can be tuned by external gate voltages by tuning the electric field in the  $z$ -direction. For example, we consider the parameters corresponding to the etched InGaAs/GaAs materials [45]:  $m^* = 0.063m_e$  and  $\beta = 10.8meVnm$ . This value is obtained from the bulk Dresselhaus constant ( $\beta_b$ ) as  $\beta = (\pi/d)2\beta_b$ , where  $d = 5nm$  is the height of the structure in the growth direction and  $\beta_b = 27.5eV\text{\AA}^3$  for GaAs [46]. Also, we consider all energies are measured in the units of the hopping energy between neighboring ( $t=1$ ) and  $a = 10nm$  as the lattice constant and number of sites in the ring  $N = 99$  and the radius of the ring is  $\sim 102nm$ .

Fig. 1 shows the tunneling magnetoresistance (TMR) functions of the electron Fermi energy for various values of magnetization. Calculations show that TMR increases with the increasing strength of the magnetization. In the absence of SOIs and small quantities of magnetization, there is no difference between conductivity in the ferromagnetic state (P) and antiferromagnetic state (P) (AP). This condition is shown in the first diagram, in which this width the value of TMR goes to zero and has its minimum value relative to other values of magnetization. But, by the first to the last diagram with increasing the strength magnetization (M), the amplitudes of conductivity in the ferromagnetic state (P) and antiferromagnetic state (AP) are increased and their degeneration is increasing. Indeed, when the outgoing interface layer is parallel to the magnetic field strength is low, and when the antiparallel to the magnetic field strength is increased. The origin of this difference is in energy bands of magnetic nanoparticles. Although, with increasing the strength magnetization (M), the TMR is increasing but the TMR strength is not in high values (TMR=1) in absence of SOIs and magnetic flux. Therefore, for achieving a perfect system with maximum TMR strength, we should consider effects of RSOI and DSOI in the presence of magnetic flux. To see the relationship between the TMR and the size of the SOIs, we first calculated the TMR of three-terminal mesoscopic ring with the presence of both DSOI and RSOI. However, verifying this conclusion needs a spacious search in  $\{t^R, t^D, E, \phi\}$  parameter space; we searched the specific values of RSOI and DSOI strengths, for which our system acts with maximum values of TMR.

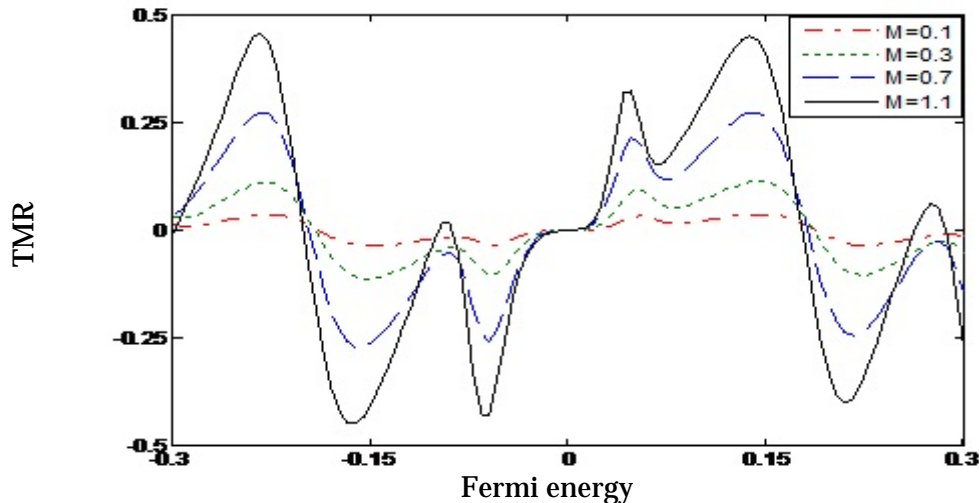


Fig. 1: TMR versus the Fermi energy for various values of  $M$  in absence of SOIs and magnetic flux

In Fig. 2 is shown the contour map of TMR plotted in  $t^D-t^R$  plane for strongly Fermi energy with  $E=0.252$  for various values of magnetization (M). Also, the values of the magnetic flux have

been tuned to be equal to 0.42. As we see in Fig. 2, by increasing magnetization peaks of the tunnel magnetoresistance shift to large values and that the system under consideration has a sharp peak of TMR only when the difference between  $t^R$  and  $t^D$  is small. Note, that the maximums and minimums of TMR occur at same specific values of  $(t^R, t^D)$  and these specific values are  $(t^R=0.32; t^D=0.33)$  for all panels. In such points TMR=0.08; 0.3; 0.7; 0.99 for weakly magnetization to strongly magnetization  $M=0.1; 0.3; 0.7; 1.1$  respectively. This behavior is obeyed also for other values of AB magnetic flux (is not shown). Therefore, for a fixed AB flux, there are specific values of both  $t^R$  and  $t^D$  with small differences for which our system looks perfectly TMR for one spin channel while totally opaque for the other spin channel and the magnetization strength has a significant role on the tunnel magnetoresistance in all configuration. So far, we have studied TMR for  $E=0.225$  with different values of  $t^R$  and  $t^D$ . Now we seek other values of  $E$  (still with same values of magnetic flux) with values of  $t^R$  and  $t^D$ , that we calculated on Fig. 2, lead to TMR=1.

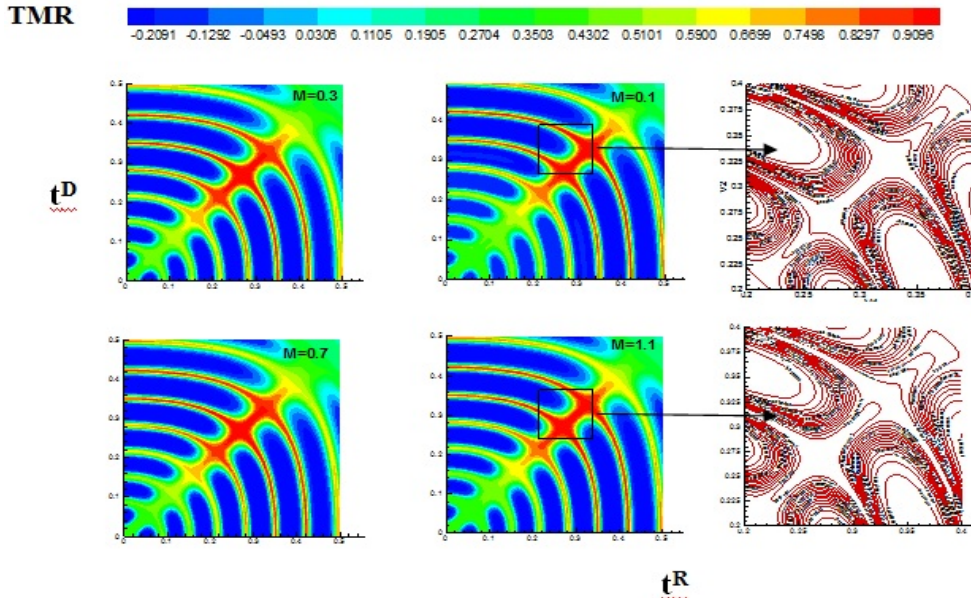


Fig. 2: (Color online) contour plot of tunnel magnetoresistance in  $t^D - t^R$  plane for various values of  $M$  in  $E=0.225$  and  $\varphi = 0.42$ . The right panels show a close up of the middle panels in the area inside the black rectangular, where the tunnel magnetoresistance has maximum values.

Fig. 3 shows the TMR current as function of the electron Fermi energy for fixed non-vanishing values of SOIs and AB flux ( $t^R=t^D=0.32; \varphi = 0.42$ ) and various values of magnetization strength. In the presence of SOIs, the degeneracy between the conductivity in the ferromagnetic state (P) and antiferromagnetic state (AP) with increasing magnetization is removed, and there is a modulation in the difference between in the ferromagnetic state (P) and antiferromagnetic state (AP) conductance. Note, that the Rashba constant can be tuned by changing the perpendicular electric field. As we see in Fig. 3, the maximum of TMR with TMR=1 occurs at Fermi energy  $E=0.252$ .

It seems that the presence of both SOIs and the magnetic flux is necessary in order to a symmetric three-terminal clean AB ring acts a perfect system with high TMR, but the presence of both RSOI and DSOI is not necessary for this system. However, verifying this conclusion needs a spacious search in all parameters. We search the specific values of  $E$  and  $t^R$  for which the perfect system conditions are established. Fig. 4 shows a contour plot of TMR as a function of both the electron energy and the DSOI strength for  $t^D=0$  (upper panels) and  $t^D=0.1$  (lower panels). In the upper panels we have compared the contour maps of TMR for  $\varphi = 0.1$  (left panel) and  $\varphi = 0.42$  (middle panel). The similar comparison has been done in the lower panels. In the left panel there is no TMR=1, while in middle panels we observed TMR=1 at specific values of  $(E, t^R)$  and some periodic values. These special values are  $(E=0.04; t^R=0.18)$  and  $(E=0.24; t^R=0.19)$  for upper panel and lower middle panel. The right panels in Fig. 4 show a close up of the middle panels in the area inside the black rectangular, and show that TMR reaches unity at these specific values.

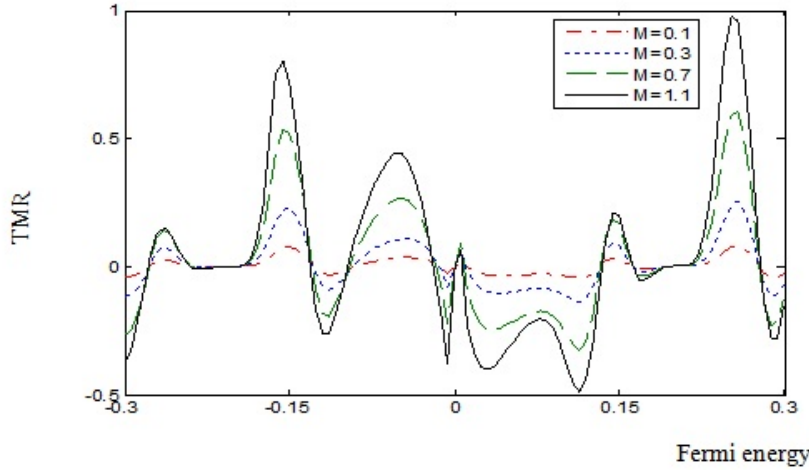


Fig. 3: The tunneling magnetoresistance in terms of the Fermi energy for various values of magnetization. Here, the specific values of  $t^R=t^D=0.32$  and  $\varphi = 0.42$  are chosen in order to get maximum values of TMR at zero conductance energies.

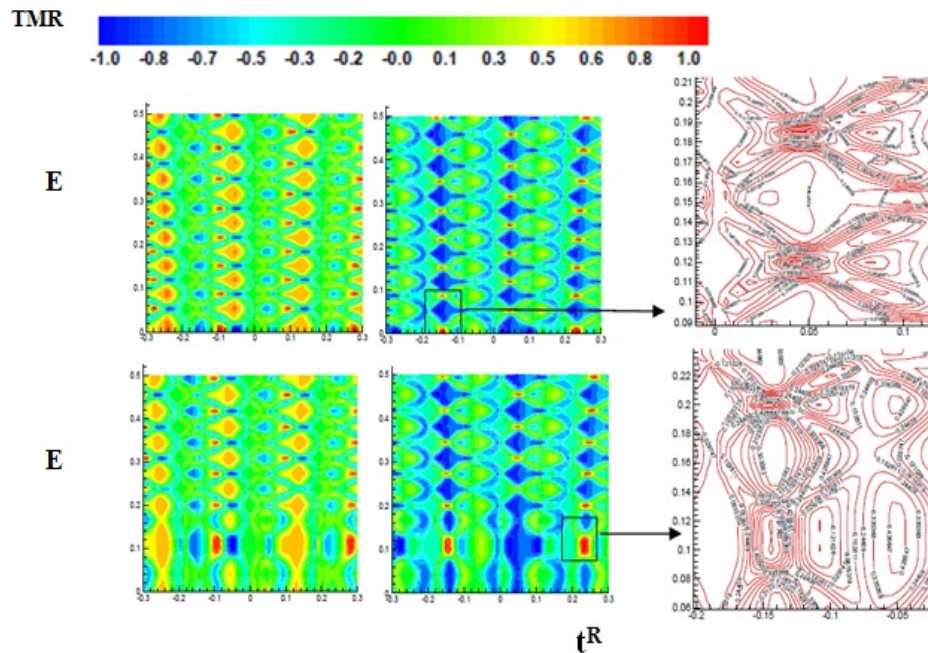


Fig. 4: (Color online) contour plot of TMR in  $E-t^R$  plane for  $t^D=0$  (upper panels) and  $t^D=0.1$  (lower panels). The right panels show a close up of the middle panels in the area inside the black rectangular, where the TMR values are equal to 1.

### Summary and conclusion

In summary, we studied the influence of the Rashba and Dresselhaus spin-orbit interaction on the tunneling magnetoresistance in a clean AB ring symmetrically coupled to the one input and two output leads. Our analysis is focused on the effect of both of the RSOI and DSOI simultaneously, which is the case in practice. Indeed, in a clean AB ring coupled symmetric to reservoirs, the presence of only one type of SOIs is necessary to reach the TMR values equal to 1. We think that such a system can act as a perfect system of TMR with unit efficiency only in the presence of RSOI and the magnetic flux. By appropriate tuning of RSOI strength by external gate voltage with respect to DSOI strength [47–50], our system serves as a perfect system of tunneling magnetoresistance at a fixed AB magnetic flux.

**References:**

1. G.A. Prinz. Magnetolectronics. *Science* 282, 1660 (1998).
2. S.A. Wolf, D.D. Awschalom, R.A. Buhrman, J.M. et al. Spintronics: A Spin-Based Electronics Vision for the Future. *Science*, 294, 1488 (2001).
3. L. Jacak, P. Hawrylak, A. Wojs. *Quantum Dots*. – New York: Springer-Verlag, 1998.
4. M. Jullier`e. *Phys. Lett.* 54 A, 225 (1975).
5. S. Maekawa, S. Takahashi, H. Imamura. In *Spin Dependent Transport in Magnetic Nanostructures*, S. Maekawa & T. Shinjo, eds. – New York: Taylor and Francis, 2002, pp. 143–236.
6. J.C. Slonczewski. *Phys. Rev. B* 39, 6995 (1989).
7. I. Žuti`c, J. Fabian, S. Das Sarma. *Rev. Mod. Phys.* 76, 323 (2004).
8. J. Fabian, A. Matos-Abiague, C. Ertler, P. Stano, I. Žuti`c. *Acta Phys. Slovaca* 57, 565 (2007).
9. S. Datta, B. Das. *Appl. Phys. Lett.* 56, 665 (1990).
10. T. Koga, J. Nitta, H. Takayanagi, S. Datta. *Phys. Rev. Lett.* 88, 126601 (2002).
11. J. Schliemann, J.C. Egues, D. Loss. *Phys. Rev. Lett.* 90, 146801 (2003); J.C. Egues, G. Burkard, D. Loss. *Appl. Phys. Lett.* 82, 2658 (2003).
12. P. Stefański. Tunneling magnetoresistance anomalies in a Coulomb blockaded quantum dot. *Phys Rev B*. 79, 085312 (2009).
13. E.I. Rashba. *Sov. Phys. Solid State* 2, 1109 (1960).
14. G. Dresselhaus. *Phys. Rev.* 100, 580 (1955).
15. J. Schliemann, J.C. Egues, D. Loss. *Phys. Rev. Lett.* 90, 146801 (2003); J.C. Egues, G. Burkard, D. Loss. *Appl. Phys. Lett.* 82, 2658 (2003).
16. H. Riechert, S.F. Alvarado, A.N. Titkov, V.I. Safarov. *Phys. Rev. Lett.* 52, 2297 (1984).
17. M. Cardon, N.E. Christensen, G. Fasol. *Phys. Rev. B* 38, 1806 (1988).
18. J. Nitta, T. Akazaki, H. Takayanagi, T. Enoki. *Phys. Rev. Lett.* 78, 1335 (1997).
19. F. Wan, M.B.A. Jalil, S.G. Tan. *J. Appl. Phys.* 105, 704 (2009).
20. L. Cai, Y.C. Tao, J.G. Hu, G.J. Jin. *Phys. Lett. A* 372, 5361 (2008).
21. S.A. Wolf et al. *Science* 294, 1488 (2001).
22. S. Urazhdin, N.O. Birge, W.P. Pratt, Jr. J. Bass. *Phys. Rev. Lett.* 91, 146803 (2003).
23. Y.X. Li, Y. Guo, B.Z. Li. *Phys. Rev. B* 71, 12406 (2005).
24. S. Urazhdin et al. *J. Appl. Phys.* 97, 10C701 (2005).
25. M. Julliere. *Phys. Lett. A*. 54, 225 (1975).
26. J. Mathon, A. Umersky. *Phys. Rev. B* 63, 220403 (2001).
27. Y. Aharonov, D. Bohm. *Phys. Rev.* 115, 485 (1959).
28. Y. Aharonov, A. Casher. *Phys. Rev. Lett.* 53, 319 (1984).
29. H.A. Engel, D. Loss. *Phys. Rev. B* 62, 10238 (2000).
30. A.G. Aronov, Y.B Lyanda-Geller. *Phys. Rev. Lett.* 70, 343 (1993).
31. Cheng-Long Jia, Shun-Jin Wang, Hong-Gang Luo, Jun-Hong An. *J. Phys.: Cond. Matt.* 16, 2043 (2004).
32. D. Frustaglia, M. Hentschel, K. Richter. *Phys. Rev. Lett.* 87, 256602 (2001).
33. R. Ionićoiu, I. Damico. *Phys. Rev. B* 67, 041307(R) (2003).
34. M.J. Gilbert, J.P. Bird. *Appl. Phys. Lett.* 77, 1050 (2000).
35. M. Popp, D. Frustaglia, K. Richter. *Nanotechnology* 14, 347 (2003).
36. S. Ikeda et al. *Appl. Phys. Lett.* 93, 082508 (2008).
37. L. Cai, Y.C. Tao, J.G. Hu, G.J. Jin. *Phys. Lett. A* 372, 5361 (2008).
38. R.S. Patel, S.P. Dash, M.P. de Jong, R. Jansen. *J. Appl. Phys.* 106, 016107 (2009).
39. C.P. Moca, D.C. Marinescu. *J. Phys.: Condens. Matter* 18, 127 (2006).
40. S.K. Maiti, M.Dey, S. Sil, A. Chakrabarti, S.N. Karmakar. *Euro-Phys. Lett.* 95, 57008 (2011).
41. S. Datta. *Electronic Transport in Mesoscopic Systems*. – New York: Cambridge University Press, 1997.
42. R. Landauer. *Phys. Lett. A* 85, 91 (1986).
43. M. Wang, K. Chang. *Phys. Rev. B* 77, 125330 (2008).
44. M. Bayer, M. Korkusinski, P. Hawrylak, T. Gutbrod, M. Michel, A. Forchel. *Phys. Rev. Lett.* 90, 186801 (2003).
45. W. Knap, C. Skierbiszewski, A. Zduniak, et al. *Phys. Rev. B* 53, 3912 (1996).

46. S.K. Maiti. *J. Appl. Phys.* 110, 064306 (2011).
47. S.K. Maiti, S. Sil, A. Chakrabarti. *Phys. Lett. A* 376, 2147 (2012).
48. M. Studer, M.P. Walser, S. Baer, et al. *Phys. Rev. B* 82, 235320 (2010).
49. C. Yin, B. Shen, Q. Zhang, F. Xu, N. Tang, L. Cen, X. Wang, Y. Chen, J. Yu. *Appl. Phys. Lett.* 97, 181904 (2010).
50. G. Baym. *Lectures on Quantum Mechanics*. – Westview Press, 1969.